

TITLE ANTIPROTON-INDUCED ELASTIC AND INELASTIC SCATTERING AT INTERMEDIATE ENERGIES

AUTHOR(S) Wei-xing Ma, T-2 Collaborator (PRC)
Daniel D. Strottman, T-2

SUBMITTED TO The IVth Conference on the Intersections Between
Particle and Nuclear Physics, Tucson, Arizona, 24-29 May 1991

DISCLAIMER

This report was prepared as an account of work sponsored by an agency of the United States Government. Neither the United States Government nor any agency thereof, nor any of their employees, makes any warranty, express or implied, or assumes any legal liability or responsibility for the accuracy, completeness, or usefulness of any information, apparatus, product, or process disclosed, or represents that its use would not infringe privately owned rights. References herein to any specific commercial product, process, or service by trade name, trademark, manufacturer, or otherwise does not necessarily constitute or imply its endorsement, recommendation, or favoring by the United States Government or any agency thereof. The views and opinions of authors expressed herein do not necessarily state or reflect those of the United States Government or any agency thereof.

The publisher acknowledges that the U.S. Government retains a nonexclusive, royalty-free license to publish or reproduce the copyrighted material contained herein or to allow others to do so for U.S. Government purposes.

The U.S. Government requests that the publisher identify this article as work performed under the auspices of the U.S. Department of Energy.

MASTER

Los Alamos Los Alamos National Laboratory
Los Alamos, New Mexico 87545

ANTIPROTON-INDUCED ELASTIC AND INELASTIC SCATTERING AT INTERMEDIATE ENERGIES

W.-H. Ma and D.D. Strottman
Theoretical Division, Los Alamos National Laboratory
Los Alamos, New Mexico, 87545, USA

With the construction and subsequent operation of LEAR, beams of low-energy antiproton with previously unobtainable intensity and quality were possible. Elastic and inelastic scattering experiments were performed on several nuclei in both the p- and sd-shell as well as on targets of heavier mass. In the very near future experiments with antiproton having momentum of up to 2 GeV/c will be possible. It is the purpose of this brief article to report results of initial calculations of \bar{p} -nucleus scattering for energies that span this new energy region and for which the elementary $\bar{p}N$ amplitudes are known.

The Glauber model has proven capable of providing an excellent description of the low-energy \bar{p} -nucleus scattering. In this work we shall use the Glauber model, which not only is quite accurate, but requires a minimum of input data for the calculations. The amplitude for (\bar{p}, p') on a nucleus of A nucleons in the Glauber model may be written as

$$F_{M_f M_i}(q^2) = i k e^{i \Delta M \frac{\pi}{2}} \int_0^\infty b db J_{\Delta M}(qb) \Gamma_{M_f M_i}(b),$$

where

$$\Gamma_{M_f M_i}(b) e^{i \Delta M \phi_b} = \langle J_f T_f M_f | 1 - \prod_{j=1}^A (1 - \Gamma_j) | J_i T_i M_i \rangle,$$

where $\Delta M = M_i - M_f$, ϕ_b is the azimuthal angle of \vec{b} , and $\Gamma_{M_f M_i}(b)$ is the nuclear profile function resulting from evaluating the nuclear matrix element. The angular distribution is calculated by averaging over initial states and summing over final states:

$$\frac{d\sigma}{d\Omega} = \frac{1}{2J_i + 1} \sum_{M_i, M_f} |F_{M_f M_i}(q^2)|^2.$$

The single-particle profile function, Γ_j , is obtained from the $\bar{p}N$ amplitude:

$$h(q) = f^{(n)}(q) + f^{(p)}(q).$$

The superscripts (n) and (p) refer to \bar{p} -neutron and \bar{p} -proton amplitudes, respectively. The $\bar{p}N$ elementary amplitudes $f^{(N)}(q)$ are assumed to have a Gaussian form

$$f^{(N)} = \frac{i k \sigma^{(N)} (1 - i \rho^{(N)})}{4\pi} e^{-\beta^2 q^2 / 2}, \quad N = n, p,$$

where the values for σ , ρ , and β are taken from the experimental evaluations of Kaseno *et al.* and Jenn *et al.* We have assumed the \bar{p} -neutron and \bar{p} -proton interaction are the same.

The initial and final nuclear wave functions that enter our calculations were calculated as a sum of Slater determinants using a version of the Glasgow shell model code. The nuclei ^{16}O and ^{40}Ca are treated as closed-shell nuclei for which there is a single determinant. ^{12}C is treated within the complete p-shell basis for which there are 51 determinants. The wave functions for mass twelve were obtained using the matrix elements of Cohen *et al.*

The single-particle wave functions were calculated assuming a Woods-Saxon central potential and binding the nucleons at their experimental energies. The single-particle wave functions were then expanded in terms of three-dimensional Hermite polynomials, for which the matrix elements of the profile function are easily calculated.

The values of the total $\bar{p}N$ cross section, σ , the ratio of the real-to-imaginary $\bar{p}N$ forward amplitude, ρ , and the value of the diffraction-slope parameter, β , used in our calculations are given in the following table.

$p(\text{GeV}/c)$	$T(\text{GeV})$	$\sigma(\text{fm}^2)$	ρ	$\beta(\text{GeV})$
0.799	0.232	13.2	0.26	5.9
1.174	0.565	10.6	0.22	14.9
1.412	0.757	10.0	0.24	14.2
1.776	1.070	9.2	0.14	13.2
2.607	1.833	8.1	0.04	13.1

The calculated results are essentially independent of small variations in the value of β . Changing ρ will essentially only affect the depth of the minima, which should not be expected to be accurately reproduced in our calculations since we have omitted the Coulomb interaction. Thus, the only essential sensitivity will be due to σ . The errors on this quantity are relatively small. The principal unknowns are the values of the three parameters for the $\bar{p}n$ interaction. We have taken them to be equal to the $\bar{p}p$ interaction, an approximation that has worked quite well at lower energies.

Figs. 1-3 show results for elastic scattering of antiprotons on ^{12}C , ^{16}O , and ^{40}Ca for five kinetic energies from 0.23 to 1.83 GeV. The forward-angle cross section increases as both the target mass and the incident energy increases. The maximum energy of the antiproton with the upgraded LEAR should be intermediate between 1.07 and 1.83 GeV. Thus, even at the maximum energies, one should anticipate being able to measure the angular distribution for scattering from ^{12}C and ^{16}O out to the second minimum and perhaps the subsequent maximum. However, it will occur at the highest energies inside 20° . For ^{40}Ca one conceivably could measure past the third minima. It is in this region that effects due to the single-particle wave function and the value of the diffraction-slope parameter, β , of the $\bar{p}n$ interaction will become more pronounced. Measurement of the angular distributions for ^{16}O , ^{18}O or several of the Ca isotopes should allow one more reliably to extract the $\bar{p}n$ interaction from experiment.

In Fig. 4 are shown results at the five energies of inelastic excitation of the 2^+ excited state of ^{12}C . We have used an effective charge of $\beta = 1.5$, a value consistent with electromagnetic transitions and other hadron-induced reactions. A value of $\beta = 1$ would have resulted in angular distributions of essentially identical shape but having a magnitude of approximately two smaller. We emphasize that our approach includes one-body through A-body scattering (always with the eikonal restriction that no nucleon is struck more than once).

Although no experimental data is now available for comparison with the theoretical predictions in this paper, the present results are sufficiently reliable to be a guide for measurements in the very near future. We believe that antiproton-induced elastic and inelastic scattering on nuclei at

intermediate energies are particularly interesting. Some new and possibly unexpected phenomena may occur owing to the unique features of the many-body system. It may also produce new information on both the nuclear structure and the antinucleon-nucleon interaction, in particular the \bar{p} -neutron interaction.

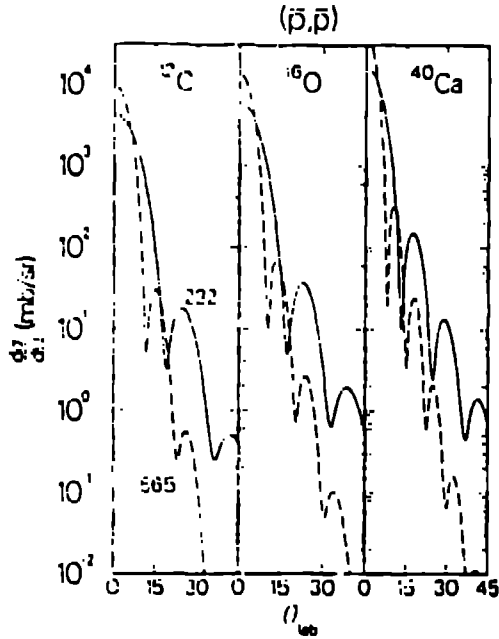


Fig. 1. Differential cross section in laboratory system for \bar{p} -elastic scattering on ^{12}C , ^{16}O , and ^{40}Ca . The solid lines are results for 232 MeV and the dashed lines for 565 MeV.

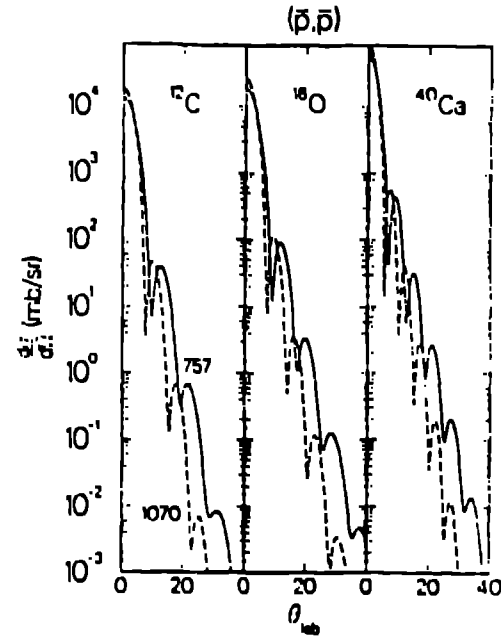


Fig. 3. Differential cross section in laboratory system for 1.83 GeV \bar{p} -elastic scattering on ^{12}C , ^{16}O , and ^{40}Ca .

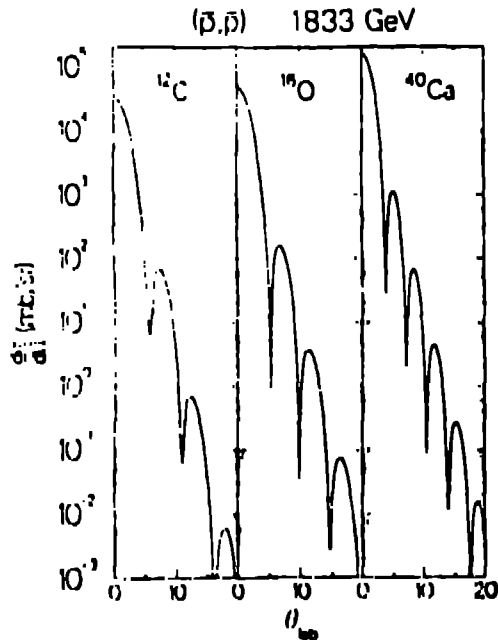


Fig. 2. Differential cross section in laboratory system for \bar{p} -elastic scattering on ^{12}C , ^{16}O , and ^{40}Ca . The solid lines are results for 757 MeV and the dashed lines for 1070 MeV.

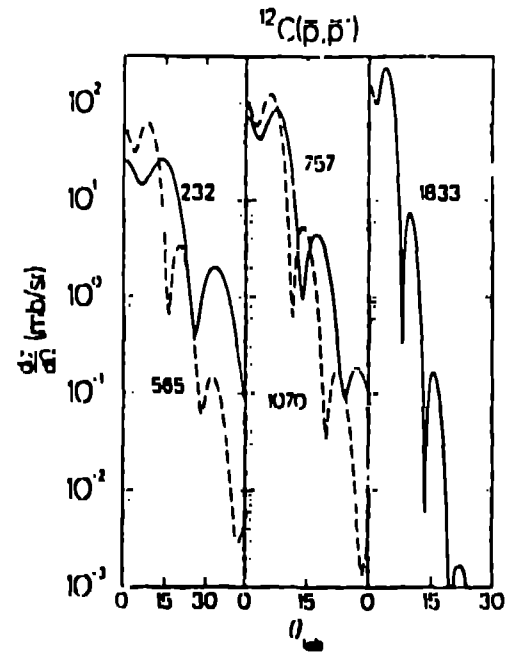


Fig. 4. Differential cross section in laboratory system for \bar{p} -elastic scattering to the 2^+ of ^{12}C at five energies. Note that the 232-MeV and 565-MeV curves extend to 45° whereas